

# Major Histocompatibility Complex Class I-ERp57-Tapasin Interactions within the Peptide-loading Complex\*

Received for publication, March 14, 2007, and in revised form, April 11, 2007 Published, JBC Papers in Press, April 24, 2007, DOI 10.1074/jbc.M702212200

Susana G. Santos<sup>‡1,2</sup>, Elaine C. Campbell<sup>‡1</sup>, Sarah Lynch<sup>‡3</sup>, Vincent Wong<sup>‡</sup>, Antony N. Antoniou<sup>§4</sup>, and Simon J. Powis<sup>‡5</sup>

From the <sup>‡</sup>Bute Medical School, University of St. Andrews, Fife KY16 9TS, Scotland, United Kingdom and <sup>§</sup>Cancer Sciences Division, University of Southampton School of Medicine, Southampton SO16 6YD, United Kingdom

The endoplasmic reticulum-located multimolecular peptide-loading complex functions to load optimal peptides onto major histocompatibility complex (MHC) class I molecules for presentation to CD8<sup>+</sup> T lymphocytes. Two oxidoreductases, ERp57 and protein-disulfide isomerase, are known to be components of the peptide-loading complex. Within the peptide-loading complex ERp57 is normally found disulfide-linked to tapasin, through one of its two thioredoxin-like redox motifs. We describe here a novel trimeric complex that disulfide links together MHC class I heavy chain, ERp57 and tapasin, and that is found in association with the transporter associated with antigen processing peptide transporter. The trimeric complex normally represents a small subset of the total ERp57-tapasin pool but can be significantly increased by altering intracellular oxidizing conditions. Direct mutation of a conserved structural cysteine residue implicates an interaction between ERp57 and the MHC class I peptide-binding groove. Taken together, our studies demonstrate for the first time that ERp57 directly interacts with MHC class I molecules within the peptide-loading complex and suggest that ERp57 and protein-disulfide isomerase act in concert to regulate the redox status of MHC class I during antigen presentation.

To bind a high affinity, optimized pool of peptides, MHC<sup>6</sup> class I molecules undergo a series of chaperone-mediated interactions within the endoplasmic reticulum (ER) (1, 2). For most MHC class I molecules, this process occurs in the multicomponent MHC class I peptide-loading complex (PLC), which in addition to  $\beta_2$ -microglobulin ( $\beta_2m$ )-associated MHC class I molecules includes the chaperone calreticulin, the oxidoreduc-

tases ERp57 and protein-disulfide isomerase (PDI), the class I-specific accessory molecule tapasin, and the peptide transporter TAP (3–5). A series of experimental reports have indicated that the PLC acts cooperatively, and that the absence of any of the components results in the disruption of MHC class I assembly, and a reduction in the efficiency of antigen presentation to T cells (6–9).

Both ERp57 and PDI are integral components of the PLC (10–12). These oxidoreductases are related to thioredoxin (TR) and share two functional CXXC motifs (denoted TR1 and TR2) (13–15). Possession of this motif permits family members to catalyze reduction, oxidation, and isomerization of disulfide bonds within substrate polypeptides (16). ERp57 normally appears to be in a GSH-dependent reduced state within the ER (17, 18), and is thus likely to be involved in reduction or isomerization reactions. However, a striking feature of ERp57 is that, in the presence of tapasin, it preferentially forms an interaction through its TR1 motif with an unpaired cysteine in tapasin at position 95 (19). The normal escape pathway that exists to release ERp57 from substrate polypeptides is inhibited by this interaction (20), leading to the whole cellular pool of tapasin being disulfide-linked to ERp57, and a large pool of cellular ERp57 being likewise occupied within the PLC (17). The reason for this sequestration of ERp57 within the PLC is not fully understood, and although in its absence MHC class I molecules appear fully oxidized, crucially there is a lack of peptide optimization (8). It therefore remains possible that ERp57 could monitor the disulfide status of MHC class I molecules through its unoccupied TR2 motif, alongside the role recently described for PDI in the oxidation of MHC class I molecules and peptide optimization within the PLC (4).

## EXPERIMENTAL PROCEDURES

**Cell Lines and Antibodies**—C58, T2, Daudi, and the .220 series cell lines were maintained in RPMI 1640 medium supplemented with 5% FBS (both Invitrogen) and with selective antibiotics where required. KG-1 cells (ECACC) were maintained in Iscove's modified Dulbecco's medium (Sigma) with 20% FBS, and were matured in the presence of 10 ng/ml PMA and 100 ng/ml ionomycin. HeLa cells were maintained in Dulbecco's modified Eagle's medium with 10% FBS. The .220 series of cells were a gift from P. Lehner (Cambridge, UK) and E. Hewitt (Leeds, UK). .220.rtpn was generated by electroporation of .220 cells with full-length rat tapasin cDNA (21) and recloned from rat C58 thymoma cells, in vector pCR3 (Invitrogen). KG-1 cells expressing cysteine mutant B\*2705 constructs were generated

\* The costs of publication of this article were defrayed in part by the payment of page charges. This article must therefore be hereby marked "advertisement" in accordance with 18 U.S.C. Section 1734 solely to indicate this fact.

<sup>1</sup> Both authors contributed equally to this work.

<sup>2</sup> Supported by Fellowship SFRH/BPD/20964/2004 from the Portuguese Foundation for Science and Technology.

<sup>3</sup> Supported by the University of St. Andrews Maitland-Ramsay Ph.D. studentship.

<sup>4</sup> Supported by Arthritis Research Campaign UK Fellowship 15293.

<sup>5</sup> To whom correspondence should be addressed. Tel.: 44-1334-463627; E-mail: sjp10@st-andrews.ac.uk.

<sup>6</sup> The abbreviations used are: MHC, major histocompatibility complex class I; TAP, transporter associated with antigen processing; MMTS, methyl methanethiosulfonate; NEM, N-ethylmaleimide; PLC, peptide-loading complex; PDI, protein-disulfide isomerase; ER, endoplasmic reticulum; PMA, phorbol 12-myristate 13-acetate; AMS, 4'-maleimidylstilbene-2,2'-disulfonic acid; DTT, dithiothreitol; PBS, phosphate-buffered saline;  $\beta_2m$ ,  $\beta_2$ -microglobulin; TR, thioredoxin; FBS, fetal bovine serum.

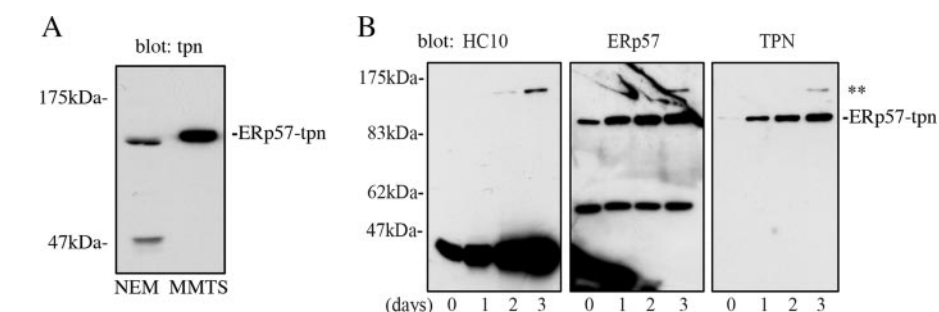


**FIGURE 1. ERp57-tapasin conjugate preservation in MMTS and detection of an MHC-ERp57-tapasin complex in KG1 cells.** A, rat C58 cells were preincubated with NEM or MMTS before preparation of detergent lysates. Samples were immunoblotted for rat tapasin. Free tapasin has a relative mass of 48 kDa, whereas the ERp57-tapasin conjugate is ~110 kDa. B, MMTS lysates of KG1 cells matured in PMA and ionomycin for the indicated times were immunoblotted for MHC class I (HC10), ERp57, and human tapasin. The ERp57-tapasin complex at 110 kDa is indicated, as is the novel complex that includes MHC class I heavy chains (\*\*), with an approximate size of 150 kDa. Longer exposures also revealed the faint presence of the novel band at day 1 and day 2 time points.

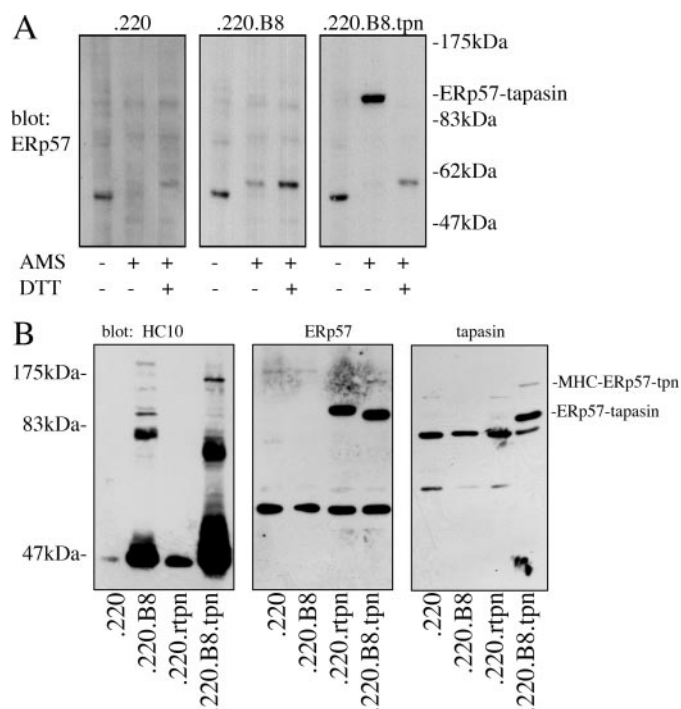


**FIGURE 2. Characterization of the MHC-ERp57-tapasin conjugate.** A, .220 series of cells were incubated with or without DTT and then treated with trichloroacetic acid and AMS to trap ERp57 intermediates. AMS (molecular mass 536.44) also slightly increases the relative size of cysteine-modified polypeptides. The ERp57-tapasin complex is indicated. In .220.B8 cells, the identical migration of DTT and non-DTT-treated ERp57 indicated that the CXXC motifs are normally in a reduced state in the ER. See also Fig. 3A. B, MMTS-treated cell lysates were immunoblotted as indicated. The ERp57-tapasin and MHC-ERp57-tapasin conjugates are indicated. The band immediately below the ERp57-tapasin conjugate in the tapasin panel is an artifact of the tapasin sera. The HC10 panel reveals potential dimer/oligomers of HLA-B8 in the 80-kDa region. Note that the ERp57 antisera recognize the complex of ERp57 and rat tapasin; however, the tapasin antisera used in this experiment is specific for human tapasin.

by electroporation. HeLa cells were transfected using FuGENE 6 (Roche Applied Science) and selected in 0.5 mg/ml G418. Monoclonal antibody HC10 recognizes unfolded HLA-B and C molecules. Anti-ERp57 was a gift from N. Bulleid (Manchester, UK). Anti-human tapasin was a gift from T. Elliott (Southampton, UK). Anti-mouse/rat tapasin was a gift from T. Hansen (St. Louis, MO). Monoclonal antibody 148.3 recognizes human TAP1. Anti-PDI was obtained from StressGen (SPA-890).

**Cell Lysates and Immunoprecipitations**—For alkylation treatments, cells were resuspended in ice-cold PBS containing 10 mM NEM (Sigma) or MMTS (Pierce) for 5 min, followed by lysis for 10 min in ice-cold 1% Nonidet P-40 containing buffer (150 mM NaCl, 10 mM Tris, pH 7.6, 1 mM phenylmethylsulfonyl fluoride, plus 10 mM NEM or MMTS). Insoluble material was removed by a 5-min centrifugation at 20,000 × g, and supernatants were heated in nonreducing sample buffer. Where indicated cells were incubated for 10 min at 37 °C with 1 mM diamide (Sigma) or 2

mm DTT prior to processing. The acid-trapping method using trichloroacetic acid has been described previously (17). For isolation of the TAP complex, 20 million cells were pretreated with MMTS in PBS and lysed in buffer as above containing 0.5% digitonin (Wako). TAP complexes were isolated using antibody 148.3 chemically cross-linked to protein G-Sepharose beads (Sigma). After extensive washing, beads were heated in nonreducing sample buffer. For metabolic labelings, cells were preincubated in methionine-free RPMI for 20 min and then labeled with 7.2 MBq of Tran<sup>35</sup>S-label (MP Biologicals) for 20 min at 37 °C. 1 mM diamide was included for the last 5 min, and the cells were then treated with MMTS in PBS, lysed, and immunoprecipitated as above. Samples were run nonreduced on SDS-PAGE and processed for autoradiography.

**Immunoblotting**—Samples were separated by 8% SDS-PAGE, transferred to nitrocellulose (BA85, Schleicher & Schuell), and blocked with skimmed milk powder in PBS plus 0.1% Tween 20 (Sigma). Primary antibodies were incubated with membranes overnight at 4 °C or for a minimum of 1 h at room temperature. Blots were developed by chemiluminescence, using SuperSignal Femto and the included horseradish peroxidase-anti-rabbit and mouse IgG reagents (Pierce).

**Mutagenesis of HLA-B\*2705**—A C-terminally tagged (V5) cDNA encoding the HLA-B\*2705 allele, cloned into the mammalian expression vector pCR3.1 (Invitrogen), was mutated using PCR-based site-directed mutagenesis (Quikchange, Stratagene) to alter conserved cysteine residues to serine or to introduce a stop codon after residue 339.

## RESULTS

**Alkylation with MMTS Reveals a Novel High Molecular Weight Species in KG-1 Cells**—The majority of studies of the PLC have involved either the use of *N*-ethylmaleimide (NEM) to alkylate unpaired cysteines (15, 19), thereby trapping ERp57-tapasin complexes, or rapid acidification to prevent thiol exchange, followed by alkylation (17). However, Cresswell and co-workers (20) have recently demonstrated that methyl methanethiosulfonate (MMTS) can also preserve the ERp57-tapasin conjugate, a result we confirm here in cell lysates of the rat C58 thymoma cell line (Fig. 1A). We used MMTS to study the for-

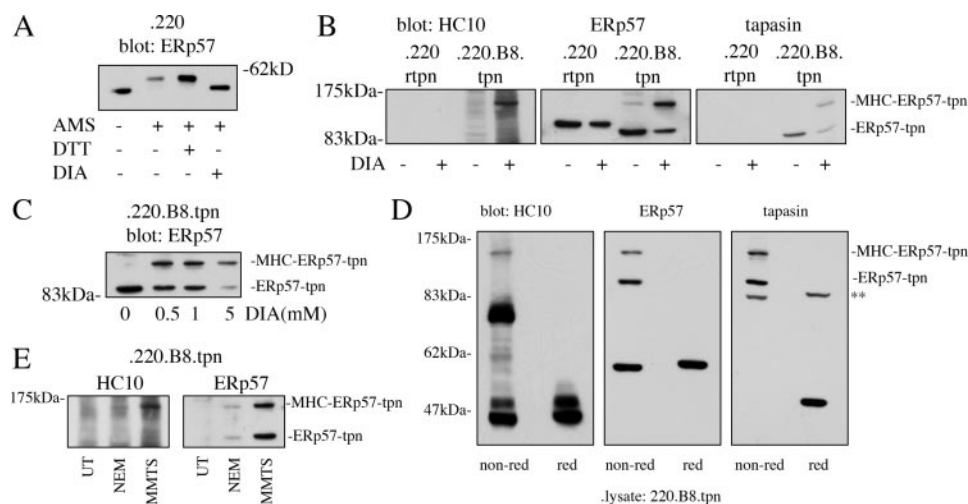


**FIGURE 3. Diamide enhances the MHC-ERp57-tapasin interaction.** *A*, .220 cells were treated with DTT or diamide (DIA), then trichloroacetic acid-precipitated, and alkylated with AMS. Diamide is shown to prevent access of AMS by oxidizing the CXXC motifs. *B*, .220.rtpn and .220.B8.tpn cells were pretreated with or without diamide before preparation of MMTS detergent lysates. Samples were then immunoblotted with HC10 or anti-ERp57 or anti-human tapasin reagents. Diamide is shown to significantly increase the MHC-ERp57-tapasin conjugate. *C*, .220.B8.tpn cells were incubated with the indicated concentrations of diamide for 10 min at 37 °C and then subsequently treated with MMTS, and lysates were prepared and immunoblotted for ERp57. *D*, diamide- and MMTS-treated cell lysates were prepared from .220.B8.tpn cells, analyzed under nonreducing (nonred) and reducing (red) conditions and immunoblotted for MHC class I, ERp57, and tapasin. The MHC-ERp57-tapasin and ERp57-tapasin bands in each case resolve to a single species under reducing conditions. The tapasin panel also reveals the nonspecific species detected just beneath the ERp57-tapasin band, labeled \*\* in this figure. This is the same species shown in Fig. 2*B* and reported in the main text. This species does not significantly alter mobility upon reduction, whereas tapasin reduces to a single species of 48 kDa. *E*, .220.B8.tpn cells were treated with 1 mM diamide, then soaked in PBS, and lysed in detergent buffer supplemented with NEM or MMTS as indicated. Lysates were probed for MHC class I and ERp57. UT, untreated.

mation of the PLC in the dendritic like cell line KG-1. KG-1 cells were matured in PMA and ionomycin for up to 3 days and MMTS-treated detergent lysates prepared. As maturation progressed, we detected a novel species with a size of ~150 kDa, which immunostained with anti-HLA-B- and -C-specific antibody HC10 and also ERp57 and tapasin specific antisera (Fig. 1*B*). This would be the expected approximate size of a disulfide-linked species containing MHC class I (43–45 kDa), ERp57 (57 kDa), and tapasin (48 kDa). The 150-kDa species was not revealed by anti-PDI, ERp72, or calreticulin antisera (not shown). Therefore, the results suggested the existence of an MHC class I heavy chain-ERp57-tapasin complex in these cells.

**Characterization of MHC Class I-ERp57-Tapasin Complex in Transfectants of the .220 Cell Line**—In a further analysis we made use of the tapasin-deficient .220 cell line (22) and stable transfectants .220.B8 (expressing HLA-B8) (23), .220.rtpn (expressing rat tapasin), and a double transfectant with B8 and human tapasin (.220.B8.tpn). As shown in Fig. 2*A*, using trichloroacetic acid-based rapid acidification and alkylation with 4'-maleimidylstilbene-2,2'-disulfonic acid (AMS), which increases the size of each nondisulfide-linked cysteine residue by ~0.5 kDa, the ERp57-tapasin complex can only be detected when both ERp57 and tapasin are present, *i.e.* in .220.B8.tpn cells. Using MMTS-treated cell lysates, we clearly detected the novel MHC-ERp57-tapasin trimeric conjugate in .220.B8.tpn cells (Fig. 2*B*). The conjugate was not detected in .220.rtpn cells, likely due to the low levels of endogenous MHC class I, as shown in the HC10 panel. Note that the anti-tapasin reagent used in this experiment does not recognize rat tapasin, and thus there is no detection of the ERp57-rat tapasin conjugate in the

anti-tapasin panel, whereas the ERp57 antisera recognizes both species (note also that the ERp57-rat tapasin complex migrates slightly slower on SDS-PAGE). Furthermore, the anti-tapasin sera frequently recognizes a nonspecific species in the .220 cell series, which can be seen migrating at ~80 kDa (see also Figs. 3*D* and 5*A*). Thus, formation of the conjugate requires the presence of MHC class I, ERp57, and tapasin. Lysates from the .220.B8.tpn line were subsequently analyzed under reducing conditions and clearly demonstrated the disappearance of both the ERp57-tapasin and the MHC-ERp57-tapasin complex under such conditions (see Fig. 3*D*).

**Enhancement of the MHC-ERp57-Tapasin Complex under Oxidizing Conditions**—To test if we could enhance the formation of the MHC-ERp57-tapasin complex, we incubated cells with the oxidizing agent diamide, which causes oxidation of the ERp57 CXXC motifs,

rendering them inaccessible to AMS modification (Fig. 3*A*) (17). We therefore treated .220.rtpn and .220.B8.tpn cells with diamide and prepared MMTS-treated lysates. Diamide treatment significantly increased the presence of the MHC-ERp57-tapasin conjugate in .220.B8.tpn cells, with the concomitant loss of signal in the ERp57-tapasin conjugate, suggesting that the enhanced trimeric complex is derived solely from the ERp57-tapasin complex (Fig. 3*B*). A titration of diamide determined that between 0.5 and 1 mM was optimal to enhance this interaction (Fig. 3*C*), with higher concentrations (5 mM) leading to a loss of protein recovered from treated cells (not shown). Diamide-treated lysates were also analyzed under reducing conditions, demonstrating reduction of the relevant complexes (Fig. 3*D*). Thus alteration to the oxidizing environment of the ER and ERp57 increases the interaction of ERp57 with MHC class I molecules. This suggests that ERp57 is acting as an oxidoreductase on MHC class I molecules, because modifications of the intracellular redox environment will influence its interaction with its substrate.

The novel MHC-ERp57-tapasin complex described so far was reliably identified in the presence of MMTS. To address whether this complex forms only because of the inclusion of MMTS, we retested .220.B8.tpn cells using NEM and including diamide oxidation. Untreated or NEM- or MMTS-treated lysates were analyzed. As shown in Fig. 3*E*, the MHC-ERp57-tapasin complex could now be detected using NEM, although at a much lower signal strength. This important control indicates that the MHC-ERp57-tapasin conjugate is not induced solely by the addition of MMTS and may also demonstrate why it has not been observed previously. Using diamide we can also detect



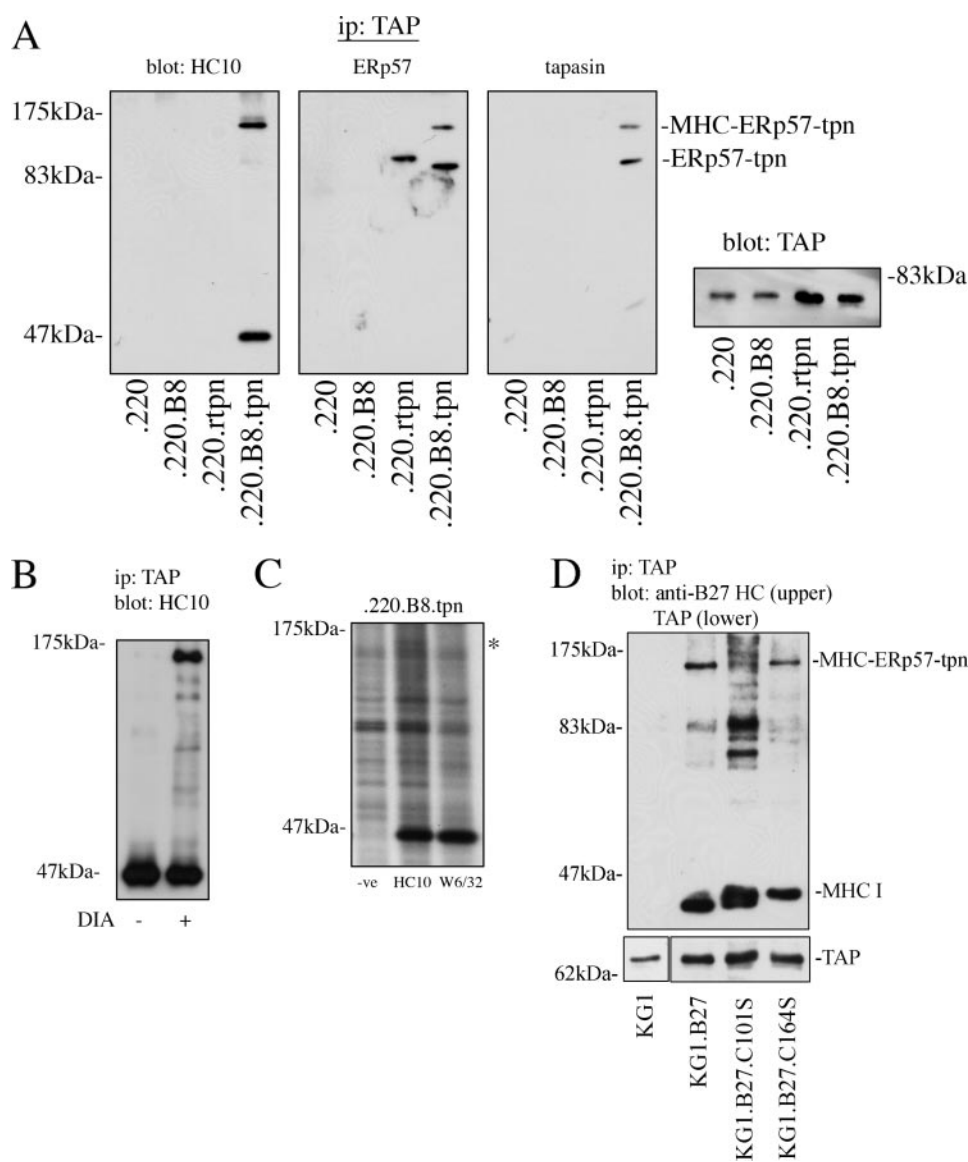


**FIGURE 4. The MHC-ERp57-tapasin conjugate is TAP-associated and is recognized by antibody HC10.** A, indicated cells were pretreated with diamide and MMTS and lysed in digitonin lysis buffer. TAP complexes were immunoprecipitated, and the sample was immunoblotted for MHC class I (HC10), ERp57, and human tapasin. The MHC-ERp57-tapasin conjugate is clearly detected in association with TAP. Rat tapasin alone forms an ERp57-tapasin conjugate but no larger complex. A control blot of the ERp57 panel stripped and reprobed for TAP indicates the immunoprecipitation of TAP in all samples. B, .220.B8.tpn cells were incubated with or without diamide (DIA), alkylated with MMTS in PBS, lysed in digitonin, and immunoprecipitated (ip) with anti-TAP antibody. The resulting immunoblot was stained with HC10 for MHC class I heavy chains. C, .220.B8.tpn cells were radiolabeled with  $^{35}\text{S}$ -label for 20 min, diamide- and MMTS-treated, lysed, and immunoprecipitated with antibodies HC10 or W6/32. The p150 complex, which migrates identically with the MHC-ERp57-tapasin conjugate, is indicated (\*). —ve, negative control lane, no antibody. D, digitonin lysates of KG1 cells expressing B27 or mutants B27.C101S or B27.C164S were immunoprecipitated for TAP and blotted for the presence of B27 heavy chain and TAP.

the conjugate using the trichloroacetic acid/AMS described earlier (not shown).

**The MHC-ERp57-Tapasin Complex Associates with TAP**—A crucial feature of the PLC is its formation with the TAP peptide transporter (24, 25), the main source of peptides translocated from the cytoplasm. We therefore tested whether we could detect the MHC-ERp57-tapasin conjugate bound to TAP. The .220 transfectant series were treated with diamide, alkylated in MMTS, lysed in digitonin to preserve TAP-PLC interactions, and immunoprecipitated with anti-TAP1 antibody. Immuno-

blotting revealed that the MHC-ERp57-tapasin conjugate was readily detected but only in .220.B8.tpn cells (Fig. 4A). A control blot confirmed isolation of TAP and the previously reported observation that the presence of tapasin stabilizes and increases the cellular pool of TAP (23). Additionally, because these immunoprecipitations isolate only the TAP-associated pool of MHC class I molecules, we determined by densitometry that, in the presence of diamide, ~30% of the MHC class I molecules are disulfide-linked to ERp57. Similarly, ~30% of the TAP-associated ERp57 and tapasin pool are in this trimeric complex. We also used this same experimental procedure to determine whether we could compare the amount of MHC class I molecules involved in the MHC-ERp57-tapasin complex in the absence of oxidizing stress. .220.B8.tpn cells were treated with or without diamide, alkylated with MMTS, and TAP-immunoprecipitated from digitonin lysates. Immunoblotting for MHC class I heavy chains was performed (Fig. 4B), and by comparing several different exposures, it was possible to calculate that in non-diamide-treated cells, only 1–3% of the TAP-associated MHC class I molecules resided within the MHC-ERp57-tapasin complex.

Antibody HC10 preferentially recognizes partially folded and therefore possibly peptide-empty structures, whereas W6/32 preferentially recognizes fully folded, peptide-loaded molecules. We used these antibodies to immunoprecipitate radiolabeled cell lysates from .220.B8.tpn cells that had been diamide- and MMTS-treated. Both antibodies isolated

the  $M_r$  45,000 B8 heavy chain, and in addition HC10 isolated a faint species at 150 kDa, which was identical in size when compared with immunoblots of the MHC-ERp57-tapasin conjugate (Fig. 4C). W6/32 did not isolate this species, suggesting that the HC10-reactive MHC-ERp57-tapasin species has an incompletely folded peptide groove.

To determine whether the MHC-ERp57-tapasin complex was part of redox regulation during peptide loading, we determined whether mutation of the conserved cysteines at positions 101 and 164 in the peptide-binding groove of HLA-B27

influenced formation of the trimeric complex. Mutation of these structural cysteines disrupts normal assembly and cell surface expression (not shown); therefore, transfected cells were incubated overnight at 26 °C to induce folding. The MHC-ERp57-tapasin conjugate was readily detected in TAP immunoprecipitates of KG-1 cells expressing both wild type B27 and a B27.C164S mutant, but it was not seen consistently in B27.C101S mutants, suggesting that ERp57 prefers to interact with the Cys-101 residue in the peptide groove. Of potential interest, mutant B27.C101S formed TAP-associated dimer-like structures, which may interfere with its ability to interact with ERp57 within the PLC, which is an area we are investigating further.

**The MHC-ERp57-Tapasin Conjugate Can Form Independently of TAP but Requires the Presence of  $\beta_2$ -Microglobulin**—Although the PLC is normally found in association with TAP, its components can also form in the absence of TAP (5, 26). We therefore asked if the formation of the MHC-ERp57-tapasin conjugate was critically dependent on TAP, and also whether the absence of  $\beta_2$ m would affect its formation. TAP-deficient T2 cells and  $\beta_2$ m-deficient Daudi cells were treated with diamide, and MMTS lysates were prepared and immunoblotted. The trimeric complex was detected in T2 cells, as shown in Fig. 5A, demonstrating its formation is not dependent on TAP. We also detected the presence of a faint higher mass species that immunoblotted for ERp57 and tapasin raising the possibility that ERp57 and tapasin may potentially form other complexes. In Daudi cells we did not detect any MHC class I-ERp57-tapasin conjugate, supporting a model where only  $\beta_2$ m-associated MHC class I molecules progress into the PLC. Furthermore, we observed that diamide treatment of Daudi cells inhibited formation of the ERp57-tapasin complex, suggesting that in the absence of  $\beta_2$ m-associated MHC class I molecules, the ERp57-tapasin complex is less stable and cannot survive oxidative stress.

Human tapasin contains an unpaired cysteine residue in its tail region (5). Several MHC class I heavy chains also contain unpaired cysteine residues in their cytoplasmic tail regions. Despite the normally reducing conditions of the cytoplasm, to exclude an abnormal disulfide linkage in this region we studied HeLa cells expressing a mutant of HLA-B\*2705 lacking the last 23 residues, including the unpaired cysteine. Diamide- and MMTS-treated lysates were probed with ERp57 antisera, which revealed the additional presence of a slightly smaller MHC-ERp57-tapasin complex resulting from the smaller size of the truncated B27 heavy chain (Fig. 5B).

The faint detection in Fig. 5A of an even larger species than the MHC-ERp57-tapasin conjugate led us to ask whether PDI may also be part of this complex. PDI was readily detected in DTT-reduced samples after digitonin lysate-based immunoprecipitation of the TAP complex from .220.B8.tpn cells (Fig. 5C, top panel). Furthermore, in nonreduced samples, we were able to identify, in several experiments, a species of over 200 kDa, which immunostained for MHC class I, ERp57, tapasin, and PDI (Fig. 5C, lower panel, indicated by \*\*). However, this species was not consistent in all experiments and requires further characterization.

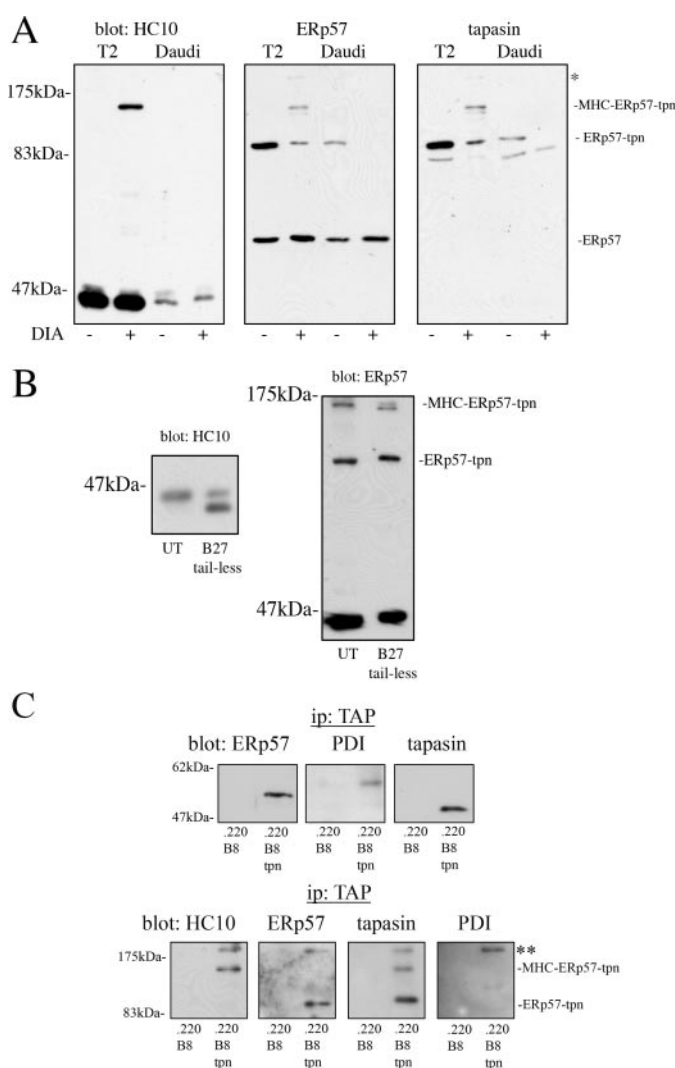


**FIGURE 5. The MHC-ERp57-tapasin conjugate does not require TAP but does require  $\beta_2$ m-associated MHC class I heavy chains.** A, T2 (TAP-deficient) and Daudi ( $\beta_2$ m-deficient) cells were treated with or without diamide (DIA) and then with MMTS and lysed, and samples were immunoblotted for MHC class I, ERp57, and tapasin. The ERp57-tapasin and MHC-ERp57-tapasin conjugates are indicated. An unidentified larger complex (\*) stains for ERp57 and tapasin but not MHC class I. B, detergent lysates of diamide- and MMTS-treated untransfected (UT) HeLa cells and cells expressing a tail-less truncated HLA-B\*2705 heavy chain were immunoprobed with HC10 and ERp57 antisera. The truncated B27 heavy chain migrates faster than endogenous HLA class I alleles, resulting in a smaller size to the MHC-ERp57-tapasin conjugate. C, .220.B8 and .220.B8.tpn cells were lysed in digitonin, and TAP immunoprecipitates (ip) were analyzed reduced (top panel) or nonreduced (lower panel) with the indicated antibodies. The complex containing PDI is indicated by a double asterisk.

## DISCUSSION

Because ERp57 was discovered as a component of the MHC class I PLC, it has been implicated in the control of the disulfide status of MHC class I molecules. Although interactions between ERp57 and MHC class I molecules have been reported (15, 27), it has not been possible to determine at what stage of the assembly process these interactions occur. Indeed, rather than readily finding MHC class I interactions, it was somewhat against expectations to find that the complete pool of ERp57 within the PLC was disulfide-bonded to tapasin (19).

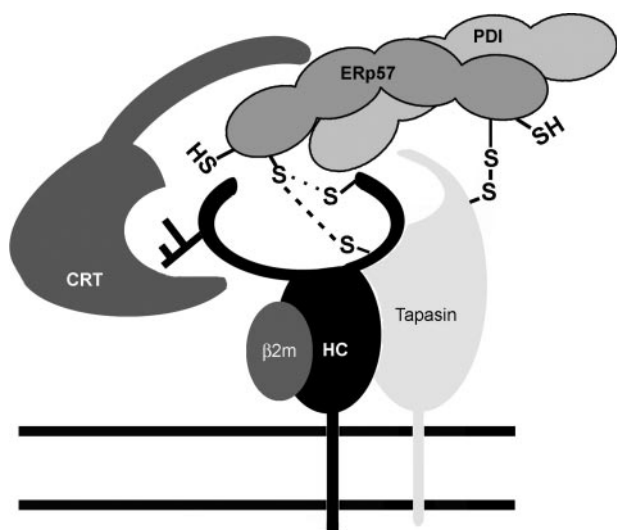


**FIGURE 6. Schematic diagram of the predicted MHC-ERp57-tapasin conjugate.** The peptide-binding groove of MHC class I contains two conserved cysteine residues involved in a disulfide bridge, at positions 101 on the groove platform and 164 in the  $\alpha 2$  helical domain. Diagram was adapted from the studies of Cresswell and co-workers (19). For clarity the potential interaction of PDI with the same cysteine residues is not indicated in this diagram. The components are labeled as follows: HC, MHC class I heavy chain; ERp57, tapasin; CRT, calreticulin.

More recently, Park *et al.* (4) have demonstrated that when PDI is incorporated in to the PLC, it potentially plays an important role in the correct oxidation of MHC class I molecules and contributes to optimal peptide selection. In contrast to the situation when ERp57 is depleted or absent (6, 8), short interfering RNA-based depletion of PDI appears to affect the oxidation status of nascent MHC class I molecules.

We have shown here that a disulfide conjugate linking MHC class I, ERp57, and tapasin exists. If, within the PLC, ERp57 is acting as a normal oxidoreductase, by forming only transient interactions with its MHC class I substrate (16), then it would be predicted that only a small proportion of the total ERp57-tapasin pool would be found in association with MHC class I. This is clearly evident in our data, for example in Fig. 2B, where the MHC-ERp57-tapasin conjugate is only a minority of the total ERp57-tapasin pool and also of the total MHC class I pool. Indeed, as we show in Fig. 4B, only a small percentage, in the range of 1–3%, of MHC class I molecules within the TAP complex interact normally with ERp57.

Based on our observations, and the recent work of others (19, 20), we hypothesize a model wherein ERp57 is capable of interacting with the disulfide bond present in the peptide-binding groove of MHC class I, depicted in schematic form in Fig. 6. In our previous studies of the actions of ERp57 upon MHC class I molecules, we developed an *in vitro* assay and demonstrated how recombinant ERp57 could act as a reductase on the partially folded HC10-reactive pool of MHC class I molecules (15). We also noted how ERp57 was more active in this role than its close relative PDI. Although we cannot distinguish with the experiments performed in this study whether ERp57 is acting as a reductase or oxidase on the MHC class I molecules with which it is interacting, based on the observations that ERp57 normally has reduced CXXC motifs *in vivo*, it is likely that it is acting as a reductase. Whether this function is required to load some

MHC class I molecules with optimal peptides or is part of a process to remove unwanted MHC class I molecules from the PLC remains to be determined.

As yet we have been unable to determine whether PDI plays a role in the formation of the MHC-ERp57-tapasin complex we describe here, although we have been able to confirm that it does co-precipitate with the TAP complex (Fig. 5C). As reported here, in some experiments we have also weakly detected a larger species, in the region of  $M_r$  200,000, which we can immunoblot for ERp57, tapasin, MHC class I and PDI.

Our data suggest a model whereby both PDI and ERp57 have access to the peptide-binding groove of MHC class I molecules during assembly within the PLC, and that they may play complementary roles in ensuring that only optimally loaded molecules egress to the cell surface. Although ERp57 is tethered to the PLC through its disulfide linkage to tapasin, it may be that PDI is a more transient visitor to the PLC, with a relatively low affinity interaction, and that its successful isolation during immunoprecipitation experiments is affected for similar reasons, thus favoring the interaction of ERp57 that we describe here. The cooperative nature of the complex may also explain why PDI has not been readily detected in cells lacking ERp57. It is clear, however, that despite our knowledge of many of the components of this pathway, our understanding of the mechanism by which each component interacts with the MHC class I molecule, and with the other parts of the PLC, remains obscure.

Some MHC class I alleles appear to be less reliant on interactions with the PLC (28), including the inflammatory arthritis-associated HLA-B27 allele, although as we have demonstrated in Fig. 4D it can interact when the PLC is available. HLA-B27 is one of a relatively rare set of MHC class I molecules that has an unpaired cysteine at position 67, pointing into the peptide-binding groove. HLA-B27 is prone to misfolding in the ER and forms disulfide-linked heavy chain oligomers, which are due, at least in part, to this additional cysteine (29–32). Thus HLA-B27 may have evolved to be less dependent on the PLC, to avoid potentially aberrant interactions between ERp57 and/or PDI, and the cysteine at position 67. We are currently investigating this possible interaction and its potential impact upon the behavior of this important disease-associated HLA allele.

*Acknowledgment*—We thank our colleagues for comments on the manuscript.

## REFERENCES

- Paulsson, K. M., and Wang, P. (2004) *FASEB J.* **18**, 31–38
- Antoniou, A. N., Powis, S. J., and Elliott, T. (2003) *Curr. Opin. Immunol.* **15**, 75–81
- Ortmann, B., Copeman, J., Lehner, P. J., Sadasivan, B., Herberg, J. A., Grandea, A. G., Riddell, S. R., Tampe, R., Spies, T., Trowsdale, J., and Cresswell, P. (1997) *Science* **277**, 1306–1309
- Park, B., Lee, S., Kim, E., Cho, K., Riddell, S. R., Cho, S., and Ahn, K. (2006) *Cell* **127**, 369–382
- Sadasivan, B., Lehner, P. J., Ortmann, B., Spies, T., and Cresswell, P. (1996) *Immunity* **5**, 103–114
- Zhang, Y., Baig, E., and Williams, D. B. (2006) *J. Biol. Chem.* **281**, 14622–14631
- Gao, B., Adhikari, R., Howarth, M., Nakamura, K., Gold, M. C., Hill, A. B., Knee, R., Michalak, M., and Elliott, T. (2002) *Immunity* **16**, 99–109



8. Garbi, N., Tanaka, S., Momburg, F., and Hammerling, G. J. (2006) *Nat. Immunol.* **7**, 93–102
9. Granda, A. G., 3rd, Golovina, T. N., Hamilton, S. E., Sriram, V., Spies, T., Brutkiewicz, R. R., Harty, J. T., Eisenlohr, L. C., and Van Kaer, L. (2000) *Immunity* **13**, 213–222
10. Hughes, E. A., and Cresswell, P. (1998) *Curr. Biol.* **8**, 709–712
11. Lindquist, J. A., Jensen, O. N., Mann, M., and Hammerling, G. J. (1998) *EMBO J.* **17**, 2186–2195
12. Morrice, N. A., and Powis, S. J. (1998) *Curr. Biol.* **8**, 713–716
13. Oliver, J. D., van der Wal, F. J., Bulleid, N. J., and High, S. (1997) *Science* **275**, 86–88
14. Oliver, J. D., Roderick, H. L., Llewellyn, D. H., and High, S. (1999) *Mol. Biol. Cell* **10**, 2573–2582
15. Antoniou, A. N., Ford, S., Alphey, M., Osborne, A., Elliott, T., and Powis, S. J. (2002) *EMBO J.* **21**, 2655–2663
16. Jessop, C. E., Chakravarthi, S., Watkins, R. H., and Bulleid, N. J. (2004) *Biochem. Soc. Trans.* **32**, 655–658
17. Antoniou, A. N., and Powis, S. J. (2003) *Antioxid. Redox Signal* **5**, 375–379
18. Jessop, C. E., and Bulleid, N. J. (2004) *J. Biol. Chem.* **279**, 55341–55347
19. Dick, T. P., Bangia, N., Peaper, D. R., and Cresswell, P. (2002) *Immunity* **16**, 87–98
20. Peaper, D. R., Wearsch, P. A., and Cresswell, P. (2005) *EMBO J.* **24**, 3613–3623
21. Deverson, E. V., Powis, S. J., Morrice, N. A., Herberg, J. A., Trowsdale, J., and Butcher, G. W. (2001) *Genes Immun.* **2**, 48–51
22. Greenwood, R., Shimizu, Y., Sekhon, G. S., and DeMars, R. (1994) *J. Immunol.* **153**, 5525–5536
23. Lehner, P. J., Surman, M. J., and Cresswell, P. (1998) *Immunity* **8**, 221–231
24. Ortmann, B., Androlewicz, M. J., and Cresswell, P. (1994) *Nature* **368**, 864–867
25. Powis, S. J. (1997) *Eur. J. Immunol.* **27**, 2744–2747
26. Paulsson, K. M., Wang, P., Anderson, P. O., Chen, S., Pettersson, R. F., and Li, S. (2001) *Int. Immunol.* **13**, 1063–1073
27. Lindquist, J. A., Hammerling, G. J., and Trowsdale, J. (2001) *FASEB J.* **15**, 1448–1450
28. Park, B., Lee, S., Kim, E., and Ahn, K. (2003) *J. Immunol.* **170**, 961–968
29. Allen, R. L., O'Callaghan, C. A., McMichael, A. J., and Bowness, P. (1999) *J. Immunol.* **162**, 5045–5048
30. Antoniou, A. N., Ford, S., Taurog, J. D., Butcher, G. W., and Powis, S. J. (2004) *J. Biol. Chem.* **279**, 8895–8902
31. Mear, J. P., Schreiber, K. L., Munz, C., Zhu, X., Stevanovic, S., Rammensee, H. G., Rowland-Jones, S. L., and Colbert, R. A. (1999) *J. Immunol.* **163**, 6665–6670
32. Tran, T. M., Satumtira, N., Dorris, M. L., May, E., Wang, A., Furuta, E., and Taurog, J. D. (2004) *J. Immunol.* **172**, 5110–5119

# **Major Histocompatibility Complex Class I-ERp57-Tapasin Interactions within the Peptide-loading Complex**

Susana G. Santos, Elaine C. Campbell, Sarah Lynch, Vincent Wong, Antony N. Antoniou and Simon J. Powis

*J. Biol. Chem.* 2007, 282:17587-17593.

doi: 10.1074/jbc.M702212200 originally published online April 24, 2007

---

Access the most updated version of this article at doi: [10.1074/jbc.M702212200](https://doi.org/10.1074/jbc.M702212200)

## Alerts:

- [When this article is cited](#)
- [When a correction for this article is posted](#)

[Click here](#) to choose from all of JBC's e-mail alerts

This article cites 32 references, 14 of which can be accessed free at <http://www.jbc.org/content/282/24/17587.full.html#ref-list-1>